LETTER • OPEN ACCESS

Magneto-optical Kerr rotation and color in ultrathin lossy dielectric

To cite this article: Jing Zhang *et al* 2017 *EPL* **118** 47006

A Letters Journal Exploring the Frontiers of Physics

May 2017

EPL, **118** (2017) 47006 www.epljournal.org
doi: 10.1209/0295-5075/118/47006

Magneto-optical Kerr rotation and color in ultrathin lossy dielectric

Jing Zhang[1], Hai Wang[1(a)], Xin Qu[2], Yun song Zhou[1] and Li na Li[3]

[1] *Department of Physics, Capital Normal University, Beijing Key Laboratory of Metamaterials and Devices, Key Laboratory of Terahertz Optoelectronics, Ministry of Education, and Beijing Advanced Innovation Center for Imaging Technology - Beijing, 100048, PRC*
[2] *Shenzhen High Trend Tech. Co., Ltd. - Shenzhen, 518129, PRC*
[3] *College of Preschool Education, Capital Normal University - Beijing, 100048, PRC*

received 28 February 2017; accepted in final form 3 July 2017
published online 27 July 2017

PACS 78.20.Ls – Magneto-optical effects
PACS 85.70.Sq – Magneto-optical devices
PACS 42.70.Gi – Light-sensitive materials

Abstract – Ultra-thin optical coating comprising nanometer-thick silicon absorbing films on iron substrates can display strong optical interference effects. A resonance peak of ∼1.6° longitudinal Kerr rotation with the silicon thickness of ∼47 nm was found at the wavelength of 660 nm. The optical properties of silicon thin films were well controlled by the sputtering power. Non-iridescence color exhibition and Kerr rotation enhancement can be manipulated and encoded individually.

The interference persists in highly absorbing films, yielding a new type of optical coating with ultrathin thickness due to the phase shifts at the boundary between lossy dielectric and air [1–10]. The non-iridescent saturated colors were evidenced in lossy germanium layers (5–20 nm thickness) deposited on gold substrate [1]. The first-order Fabry-Perot optical resonance dominated the interference in ultrathin lossy dielectric film [7,8]. Diverse absorbing materials, such as HgTe, InAs, GaAs, Ge and Si [3–10], had been reported to realize such a strong interference and its related color exhibition. However, an absorbing dielectric with the fixed optical parameters limits its optical exhibitions and applications. In our previous work [11], it is revealed by calculations that the real refractive index of dielectric plays a major role on the variations of color and Kerr signal, while the absorbing term adjusts the intensive color exhibition and Kerr enhancement at much thinner dielectric thickness.

Here, we showed that the optical properties of a silicon film are manipulated simply by the sputtering power. In a silicon/iron structure, both color exhibition and Kerr rotation were encoded and adjusted simply by the sputtering power individually. A ∼1.6° longitudinal Kerr rotation was realized at a wavelength of 660 nm with the thickness of silicon ∼47 nm, accompanying a color band transition visually. The color deviation was undetectable in a wide viewing angle with respect to the surface normal. The controllable interference in a lossy medium with a broad range optical exhibition benefits the applications of a lossy dielectric optical coating.

The silicon/iron bilayers were fabricated by DC magnetron sputtering on coverslips. The sample holders are well attached on a circulating water cooling base during deposition. The base pressure was better than 5×10^{-5} Pa. The argon flow rate was fixed as 10.0 sccm. The deposition rate of iron was 0.39 nm/s and the thickness of iron film was 100 nm. The longitudinal Kerr rotation angle (θ_K) of the bare iron film was 100 millidegree. Our experiment silicon target is from ZhongNuo Advanced Material (BeiJing) Technology Co. Limited, with the purity 99.999%. The deposition rate of silicon with the sputtering power of 36 W, 112 W, 140 W and 250 W were 0.008 nm/s, 0.025 nm/s, 0.03 nm/s and 0.046 nm/s, respectively. Film thicknesses were examined by a surface

(a) E-mail: wanghai_0410@qq.com (corresponding author)

profilometer (KLA-Tencor P10). Wedge-shaped silicon thin films (5–55 nm) were achieved by an oblique sputtering deposition method [3]. The longitudinal Kerr rotation angle was measured by NanoMOKE-III (Durham Magneto Optics Ltd.) at 660 nm with 45-degree *s*-polarized wave incidence.

Figure 1(a) shows the schematic plot of calculation model consisting of a single dielectric layer on a ferromagnetic metal, which is an asymmetric Fabry-Perot (FP) optical cavity. An incident beam polarized perpendicular to the plane of incidence gives rise firstly to a series of reflected beams, which are also polarized perpendicular to the plane of incidence. The beams within the dielectric layer produces a Kerr component polarized parallel to the plane of incidence, which subsequently suffers multiple reflections at the boundaries of the dielectric and gives a total amplitude contribution in the beam reflected from the film. The amplitude monotonically decreases with the reflecting/refracting order. Taking *s*-polarized light as an example, as the reflecting substrate is not ferromagnetic, *p*-polarized lights does not appear in the multiple reflection and refraction. However, when the reflecting substrate is ferromagnetic, reflection and refraction lights on the interfaces become new light sources for the next reflection and refraction. Both *s*- and *p*-polarized components of lights should be considered. The former represents the usual reflectance of the film for polarized light incidence, the latter represents the new *p*-polarized generating from the interfaces of dielectric/ferromagnetic [11,12].

The color, θ_K and reflectivity variation with different silicon thickness (5–55 nm) at the sputtering power of 80 W in a silicon/iron structure are shown in fig. 1(b). Color of the sample starts as yellowish brown at thinner Si thickness, follows by drab, then purple gray, and ends up as dark blue. As the reflectivity approaches to its minimum, θ_K finds its maximum (∼1.6°) around the thickness of silicon layer ∼47 nm. A big jump of θ_K, from a positive 1.6° to a negative 0.35°, is observed in the curve of θ_K *vs.* *d*. The peak and valley difference of θ_K is ∼1.95°, and the corresponding thickness difference of silicon is ∼4.3 nm. Compared to the maximum longitudinal Kerr rotation (0.1°) obtained in the bare thin iron film, the enhancement factor of θ_K is ∼16. The yellow and red solid lines in fig. 1(b) are the simulation results for θ_K and reflectivity by an asymmetric Fabry-Perot model, which match well with the experiments. The simulation parameters are illustrated in figure caption and the details can be referred to [11]. Qureshi *et al.* reported that a quite huge optical Kerr effect had been realized by 320 nm SiO_2 in infrared regime, which can explore the use of optical coatings for near-field and far-field measurements of the polar Kerr effect in small magnetic structures. For a single layer of SiN (70 nm) on nickel, a Kerr rotation increase of a factor of 5 at 785 nm wavelength, and a reduction in the size of the smallest nanomagnet that they could measure [13,14]. An enhancement θ_K at 660 nm with the ultrathin single lossy dielectric coating benefits the lateral

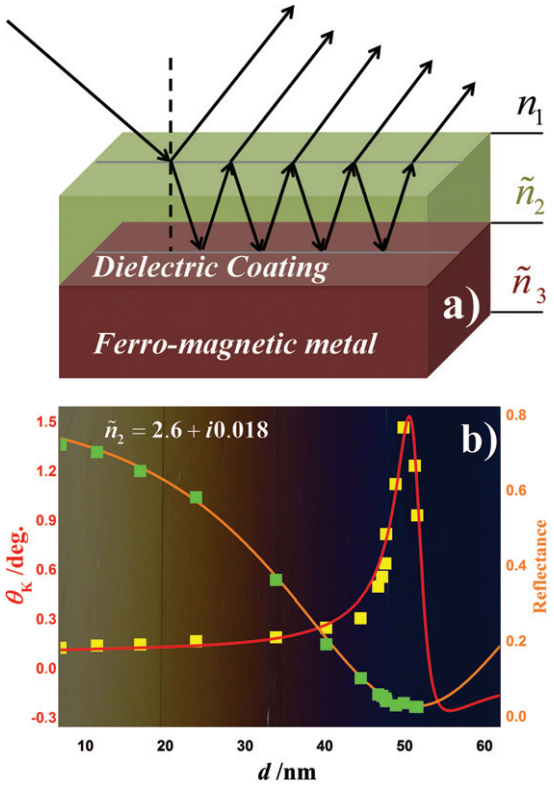

Fig. 1: (Color online) (a) The schematic plot of the calculation model: air/dielectric coating/ferro-magnetic metal. The complex refractive index of dielectric coating and magnetic metal are $\tilde{n}_2$ and $\tilde{n}_3$, respectively. (b) The experiment and simulation results of the silicon thickness as a function of θ_K and reflectivity, the background is the color of silicon/iron sample. Red and orange Solid lines correspond to the calculation of θ_K and reflectance results. Yellow and green singlet dots are the experiment of θ_K and reflectivity results, respectively.

spatial resolution improvement of ferromagnetic domain observation, due to the small modification of surface morphology as well as the high signal-to-noise ratio.

The optical properties of silicon can be adjusted by the fabrication parameters, such as the sputtering power, the chamber pressure, the substrate temperature, the flow rate of argon gas, and the target-to-substrate distance, etc. Here, we demonstrate the optical properties manipulation by the sputtering power, varying from 36 to 250 W. Two typical experimental and calculation results of θ_K with different sputtering powers are shown in fig. 2(a). As the sputtering power is 36 W, a positive peak value of θ_K (0.5°) is obtained at $d \approx 54$ nm, and then the positive θ_K reaches its maximum (1.6°) at the sputtering power of 80 W. The amplitude of θ_K falls into a negative peak valley (0.35°) at $d \approx 27$ nm with the sputtering power of 250 W. It is noted that increasing the sputtering power, the maximum θ_K with a significant sign jump appears at thinner silicon thickness.

The optical properties of silicon film rely on its complex refractive index: the real refractive index (n_2) and the absorption coefficient (k_2). Figure 2(b) shows the

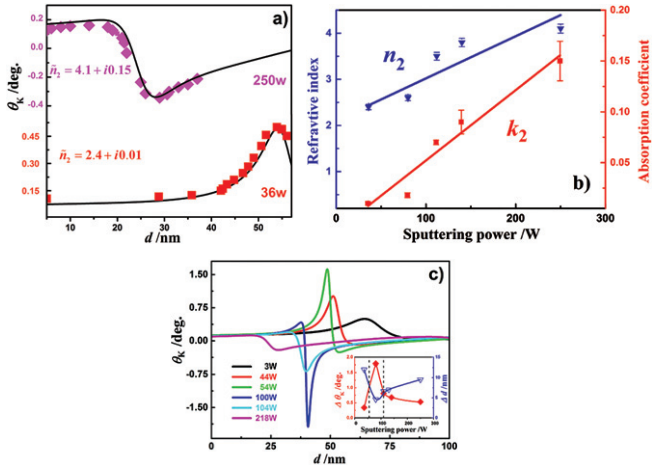

Fig. 2: (Color online) (a) Experimental and theoretical θ_K *vs.* the thickness of coating. Two different colored lines represent the θ_K spectra with the sputtering power of 36 W and 250 W, respectively. The solid lines are the theoretical results and the dot lines are the measured results. (b) The optical properties of the Si film as a function of the sputtering power. Blue and red solid lines represent the simulation of the real part of refractive index of Si and the absorption coefficient of Si, respectively. Singlet dots demonstrate the experiment results. (c) Six typical theoretical θ_K-d curves with different sputtering power. The insert plots in (c) are peak and valley difference of θ_K and the thickness difference of Si under different sputtering power.

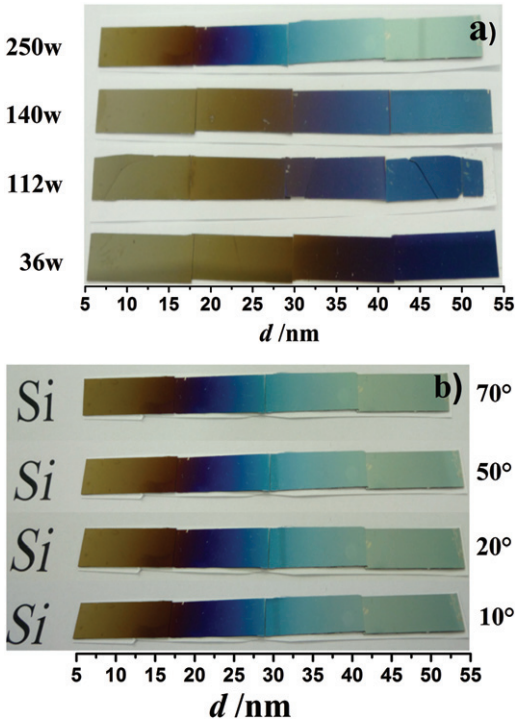

Fig. 3: (Color online) Photos of the samples comprising optically thick iron deposited on a coverslip, with a film of silicon of gradually varying thickness. (a) The color bands with the sputtering power of 36 W, 112 W, 140 W and 250 W, respectively. (b) The fabricated sample taken at different incident angles 10°, 20°, 50°, 70° with the sputtering power of 250 W.

optical properties of Si films as a function of the sputtering power. n_2 and k_2, acquired from the best simulation for θ_K-d curves at the wavelength of 660 nm, increase linearly with the increase of sputtering power ranging from 36 to 250 W. n_2 varies from 2.4 to 4.1 and k_2 changes from 0.01 to 0.15. The increase of the refractive index and the extinction coefficient are attributed to the dense uniform film. With the increase of sputtering power, the energy loss of the sputtering particles in collision with argon gas molecules reduces [15]. A set of n_2 and k_2 corresponds to a certain sputtering power. It is noted that by tuning the oxygen/argon flow rate ratio, the refractive index of dielectric film can be adjusted also. Recently, Mao *et al.* presented that in the structure of two metallic films spaced by a SiO_x dielectric layer, the absorption coefficient of SiO_x is controlled systematically to realize a new type of color filter with a broad angle insensitivity [16].

Figure 2(c) shows calculated θ_K-d spectra with six different sputtering powers. The θ_K-d curves exhibit a peak-valley characteristic, which moves to the thinner dielectric thickness with the increase of the sputtering power. As the sputtering power is lower than 54 W, the peak value dominates the feature of peak-valley structure. θ_K-d experiences a significant transition while the sputtering power is larger than 100 W, where the valley plays a major role for the θ_K-d. Between 54 and 100 W, a huge θ_K single can be achieved in a narrow dielectric thickness range due to the best impedance matching condition [11,17]. However, in view of application, a stable θ_K single of a real sample needs a certain dielectric thickness tolerance. In our experiments, the best experimental condition is achieved as: $\theta_K > 1.5°$ under ∼80 W for silicon deposition with ∼1 nm silicon thickness tolerance. The peak and valley difference of θ_K and d, derived from experiment data, are presented in the inserted plot of fig. 2(c), in which the best experimental condition regime is indicated by two black dashed lines. Recently, Daria *et al.* realized ultrahigh sensitivity detection on the environment refractive index variation by the transversal magneto-optical Kerr effect [18]. An intense magneto-optical Kerr effect (MOKE) resonance in an ultrathin lossy dielectric thin film allows for more precise thickness measurements of the MOKE resonance position and shift.

The front views of the resulting samples taken under ambient sunlight are given in fig. 3(a). The four sections correspond to different sputtering powers of silicon thin films. Each sample comprises an optically thick iron deposited on a coverslip with a film of silicon gradually varying thickness from 5 to 55 nm. As the sputtering power of silicon is 36 W, the thickness of the rainbow-like color period is 50 nm. In the case of 250 W, the rainbow-like color period is compressed to 21 nm. It is comparable with the report by Kats *et al.*, where a ∼25 nm color band exhibition has been realized by germanium ultrathin coating on the optically thick gold [1]. In addition, an ultra-thin lossy

Table 1: (Color online) Photos of blue, yellow, purple images with different θ_K at the sputtering power of 112 W, 140 W, and 250 W.

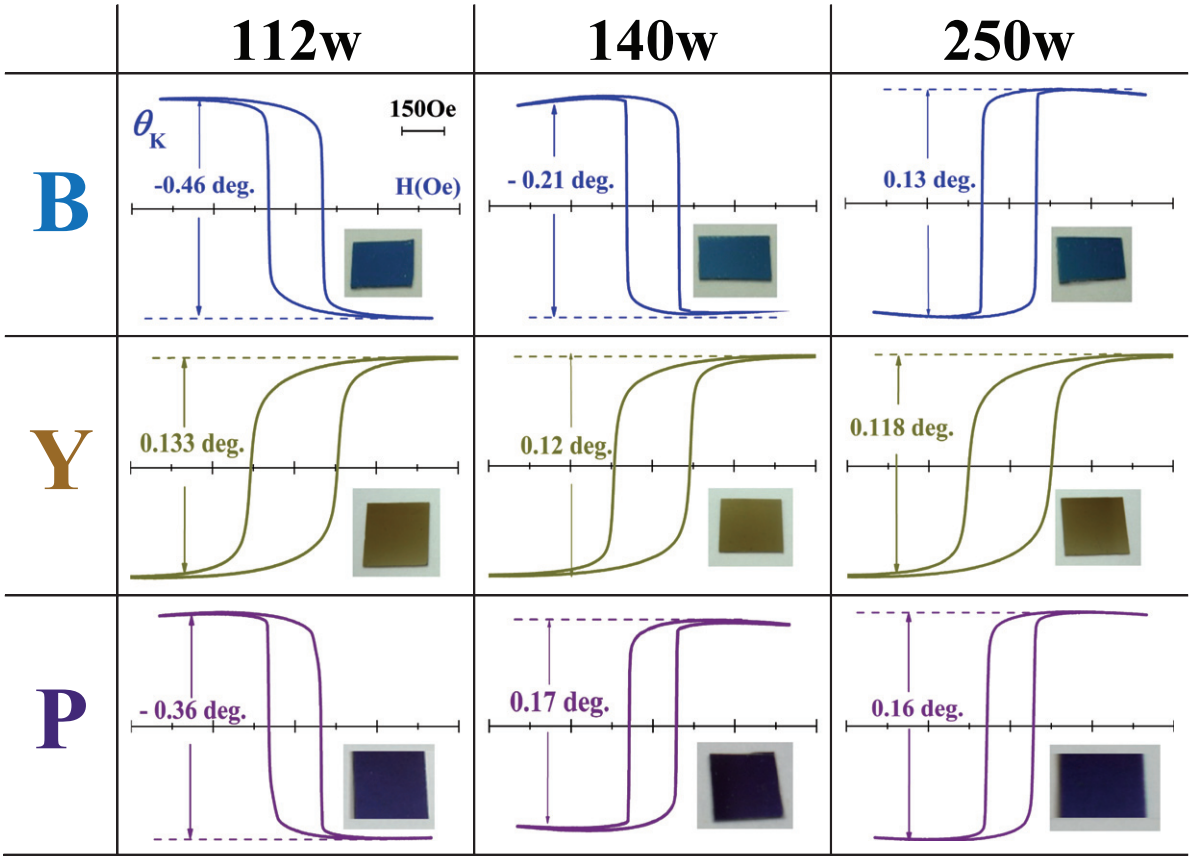

dielectric coating is significantly less sensitive to the angle of incidence. As shown in fig. 3(b), there are no observable color variations in a broad range observation angle, ranging from 0 to 70 degree. The intense interference is realized in an ultra-thin lossy dielectric film on reflecting metal substrate structure, due to the non-trivial optical phases aroused by the absorption terms accumulating at the interfaces [19–22]. Such a non-trivial phase accumulation in ultrathin film is small, yielding a wide viewing angle [2].

Table 1 demonstrates a spectrum of non-iridescence colors including blue, yellow, and purple with different θ_K by controlling the sputtering power of silicon. The sputtering powers are set as 112 W, 140 W and 250 W. As seen from table 1, yellow with the θ_K of $+0.133°$, $+0.12°$ and $+0.118°$; blue with the θ_K of $-0.46°$, $-0.21°$ and $+0.13°$; purple with the θ_K of $-0.36°$, $+0.17°$ and $+0.16°$. The advantage of our approach is that same color but different θ_K can be achieved in ultrathin lossy dielectric films (first color period) by only using the varying sputtering power method.

In summary, a $\sim 1.6°$ longitudinal Kerr rotation is reported in silicon/iron structure at the wavelength of 660 nm, which can be applied to enhance the lateral spatial resolution or improve observation sensitivity. The optical properties of silicon film are manipulated simply by the sputtering power, resulting in the Kerr rotation enhancement and non-iridescence color exhibition. The color is insensitive to the incidence angle in a broad range. The color and θ_K can be individually encoded in ultrathin lossy films by controlling the sputtering power. Some promising applications are expected, such as ultrathin domain detectors, anti-counterfeiting, information coding, solar cells, and even biochemical sensors.

* * *

This work was financially supported by the National Natural Science Foundation of China (NSFC) with Grant No. 11274233 and Beijing education committee under grant KM201610028004.

REFERENCES

[1] Kats M. A., Blanchard R., Genevet P. and Capasso F., *Nat. Mater.*, **12** (2012) 20.
[2] Kats M. A. and Capasso F., *Appl. Phys. Lett.*, **105** (2014) 131108.
[3] Kats M. A., Byrnes S. J., Blanchard R., Kolle M., Genevet P., Aizenberg J. and Capasso F., *Appl. Phys. Lett.*, **103** (2013) 101104.

[4] Kats M. A., Blanchard R., Ramanathan S. and Capasso F., *Opt. Photon. News*, **25** (2014) 40.
[5] Schlich F. F., Zalden P., Lindenberg A. M. and Spolenak R., *ACS Photon.*, **2** (2015) 178.
[6] Schlich F. F. and Spolenak R., *Appl. Phys. Lett.*, **103** (2013) 213112.
[7] Mirshafieyan S. S. and Guo J., *Opt. Express*, **22** (2014) 31545.
[8] Mirshafieyan S. S., Luk T. S. and Guo J., *Opt. Mater.*, **6** (2016) 1032.
[9] Park Junghyun, Kang Ju-Hyung, Vasudev Alok P., Schoen David T., Kim Hwi, Hasman Erez and Brongersma Mark L., *ACS Photon.*, **1** (2014) 812.
[10] Yen S.-T. and Chung P.-K., *Opt. Lett.*, **40** (2015) 3877.
[11] Zhang Jing, Wang Hai, Qu Xin, Zhou Yunsong, *AIP Adv.*, **7** (2017) 025304.
[12] Lissberger P., *J. Opt. Soc. Am.*, **51** (1961) 957.
[13] Qureshi N., Schmidt H. and Hawkins A. R., *Appl. Phys. Lett.*, **85** (2004) 431.
[14] Qureshi N., Wang S. Q., Lowther M. A., Hawkins A. R., Kwon S., Liddle A., Bokor J. and Schmidt H., *Nano Lett.*, **5** (2005) 1413.
[15] Kim K., Park M., Lee W., Kim H. W., Lee J. G., Lee C., *Mater. Sci. Technol.*, **24** (2008) 838.
[16] Mao Kening, Shen Weidong, Yang Chenying, Fang Xu, Yuan Wenjia, Zhang Yueguang and Liu Xu, *Sci. Rep.*, **6** (2016) 19289.
[17] Cantwell P. R., *J. Appl. Phys.*, **100** (2006) 093910.
[18] Ignatyeva Daria O., Knyazev Grigory A., Kapralov Pavel O., Dietler Giovanni, Sekatskii Sergey K. and Belotelov Vladimir I., *Sci. Rep.*, **6** (2016) 28077.
[19] Yang Chenying, Shen Weidong, Zhang Yueguang, Li Kan, Fang Xu, Zhang Xing, Liu Xu, *Sci. Rep.*, **5** (2015) 9285.
[20] Lee K.-T., Seo S., Lee J. Y. and Guo L. J., *Adv. Mater.*, **26** (2014) 6324.
[21] Cheong Byoung-Ho, Prudnikov O. N., Cho Eunhyoung, Kim Hae-Sung, Yu Jaeho, Cho Young-Sang, Choi Hwan-Young and Shin Sung Tae, *Appl. Phys. Lett.*, **94** (2009) 213104.
[22] Lee K. T., Seo S., Lee J. Y. and Guo L. J., *Appl. Phys. Lett.*, **104** (2014) 231112.